Singular vortices as building blocks of atmospheric low-frequency variability

Sergey Kravtsov[1,2] and Gregory Reznik[2]

[1]Department of Mathematical Sciences, Atmospheric Science Group, University of Wisconsin-Milwaukee, P.O. Box 413, Milwaukee, WI 53201

[2] P. P. Shirshov Institute of Oceanology, Russian Academy of Sciences

UNIVERSITY of WISCONSIN
UWMILWAUKEE
College of Letters and Science
ATMOSPHERIC SCIENCE
DEPARTMENT OF MATHEMATICAL SCIENCES

EGU General Assembly 2019

Session: NP1.1/AS5.19/CL5.23/HS11.33/NH11.10 – Mathematics of Planet Earth; Presentation number: X4.267; Display time: Thursday, April 11th, 14:00–15:45

Introduction

General circulation of the atmosphere is characterized by multi-scale flows with a vigorous eddy field of intense cyclones and anticyclones (synoptic eddies) that control the day-to-day weather variations, but also exhibit a pronounced low-frequency variability. Recent studies showed that the latter variability can be thought of in terms of the low-frequency redistribution of the atmospheric storm tracks, which is insensitive to the detailed spatial structure of the individual synoptic eddies (Löptien and Ruprecht 2005; Kravtsov and Gulev 2013; Kravtsov et al. 2015). This observation suggests an idea of tackling the problem of multi-scale mid-latitude atmospheric variability by considering the systems of interacting singular vortices; in such systems, the singular eddy field is clearly isolated from the regular field, thereby allowing unambiguous identification of the various dynamical components of the eddy–mean-flow interaction (Obukhov 1949; Morikawa 1960; Gryanik 1986; Reznik 1992). The same approach is applicable for studying oceanic mesoscale processes (Early et al. 2011). In this work, we develop a numerical finite-difference model describing the evolution of a singular monopole on a beta-plane and show that it provides a reasonable approximation of the continuous equations.

Numerical methodology

The governing equations (1–4) for the joint evolution of the singular streamfunction ψ_s and regular flow ψ are given by

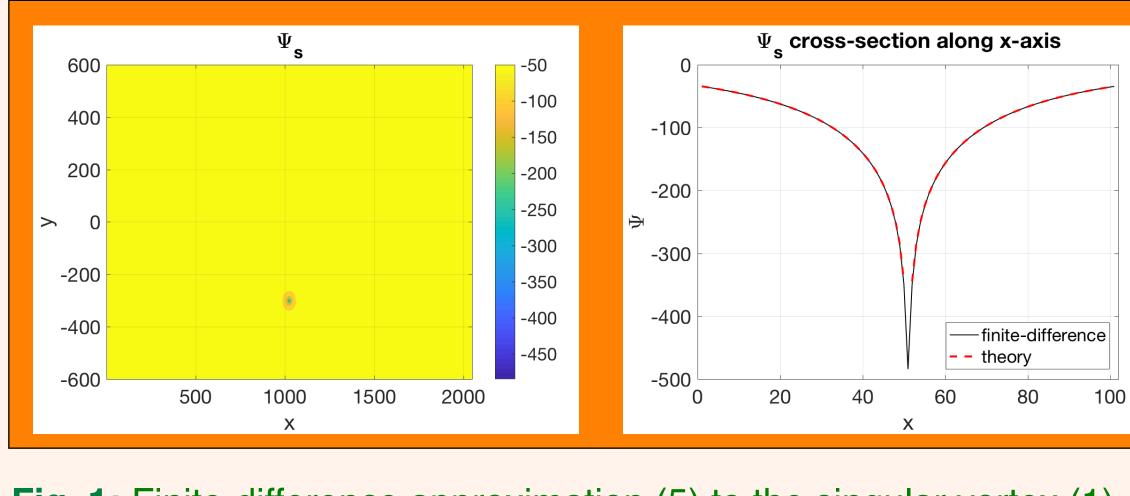$$\psi_s = -\frac{A}{2\pi}K_0(p|\mathbf{r} - \mathbf{r}_0(t)|) \qquad (1)$$

$$\partial_t \Omega + J(\psi + \psi_s, \Omega + \beta y) + (p^2 - a^2)J(\psi + U_0 y - V_0 x, \psi_s) = -K\nabla^6\psi \quad (2)$$

$$\Omega = \nabla^2\psi - a^2\psi; \; U_0 = \dot{x}_0 = -\partial_y\psi|_{r=r_0}; \; V_0 = \dot{y}_0 = \partial_x\psi|_{r=r_0}, \quad (3)$$

$$\psi|_{t=0} = 0. \qquad (4)$$

Here $a = R_d^{-1}$, R_d is the Rossby scale; $p = L_v^{-1}$, L_v is the vortex scale, A is the vortex intensity, $\mathbf{r}_0(t)$ is the vortex trajectory and K is the coefficient of horizontal superviscosity, which acts on the regular field only. In numerical formulation, the Bessel vortex (1) is replaced by its non-singular finite-difference equivalent (see Fig. 1):

$$(\psi^*_{s\,i,j+1} + \psi^*_{s\,i,j-1} + \psi^*_{s\,i+1,j} + \psi^*_{s\,i-1,j} - (4 + p^2\Delta^2)\,\psi^*_{s\,i,j})/\Delta^2 = A\,\delta_{i,io}\delta_{j,jo}/\Delta^2. \quad (5)$$

Fig. 1: Finite-difference approximation (5) to the singular vortex (1), which coincides with the Bessel vortex at all grid points except at the center of the vortex.

Salient features of singular vortex evolution

The equations (1–4) with the 'finite-difference' singular-vortex analog (5) were solved in an x-periodic domain using parameters typical for mid-latitude atmosphere for a range of vortex sizes and horizontal superviscosities. For very small friction, the singular-vortex trajectories for the point-vortex case (**Fig. 2**) are close to the numerical solution of the linearized problem, which also matches exactly the analytical solution of this problem (Reznik 1992), for times up to 30 days. In this linear regime, the system's evolution is due to the development of the so-called beta-gyres (**Fig. 3**). At later stages, the system enters inertial regime; here beta-gyres disintegrate and the regular field in the vicinity of the singular vortex becomes monopolar and offset of the singular-vortex center, resulting in the northwestward propagation.
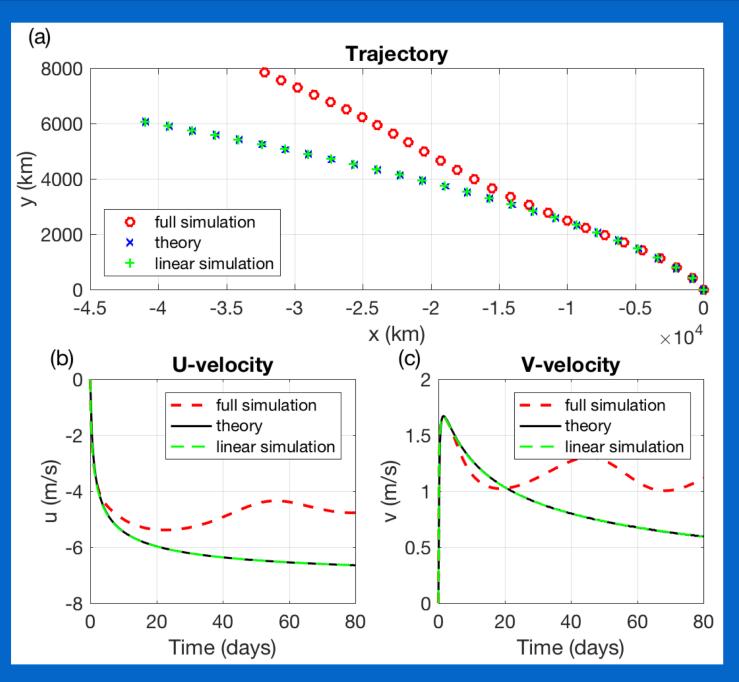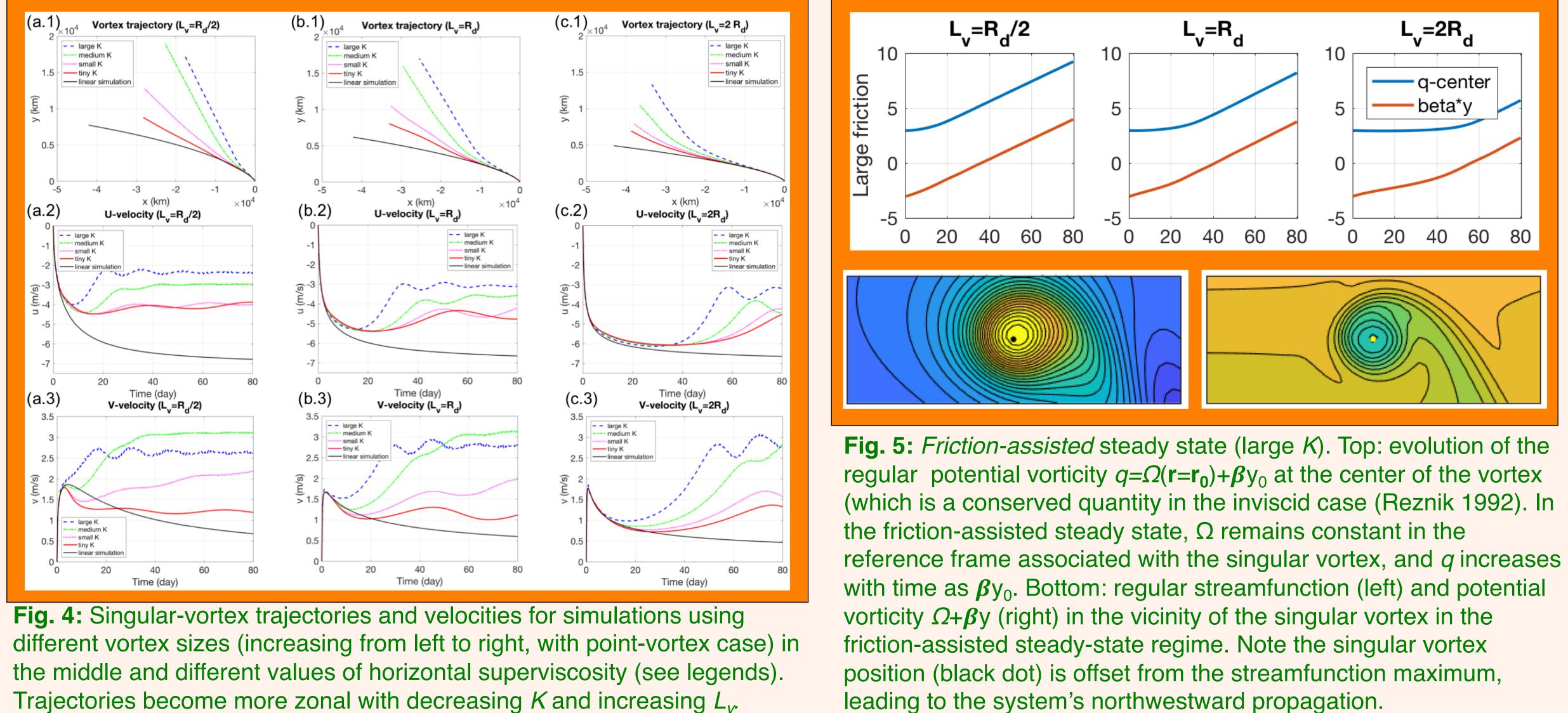

Fig. 2: Singular vortex paths (top) and velocities (bottom) for the point-vortex case $L_v = R_d = 600$ km with very small superviscosity K. The results are shown for the full-model simulation, the simulation of a linearized model in which regular-field's self-advection is neglected, and for the exact theoretical solution of the linear problem (Reznik 1992). Linear solution is close to the full solution for ~30 days or so.
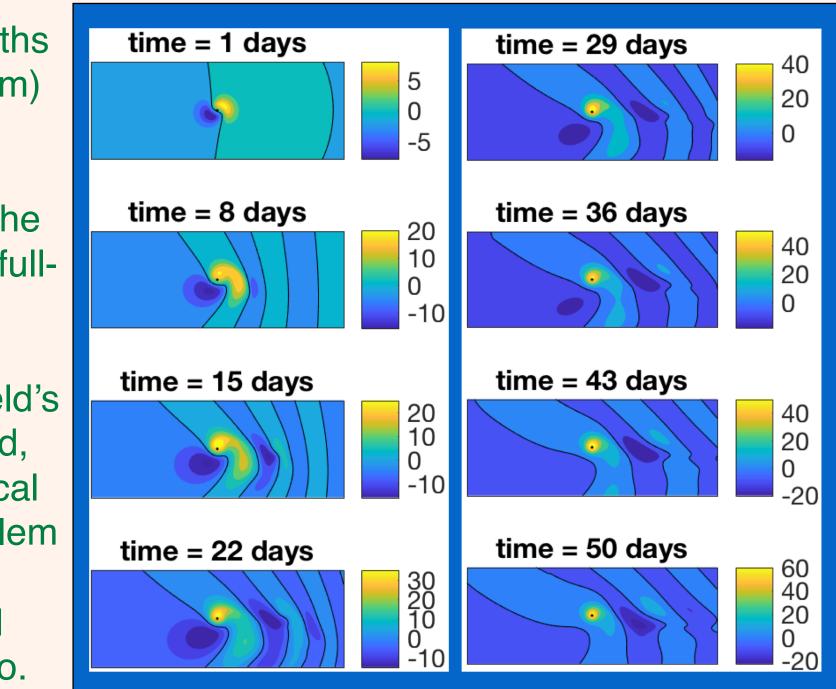
Fig. 3: The evolution of the regular stream-function for the case shown in Fig. 2. Evident is the development of the beta gyres at small times, and their subsequent disintegration, with the development of the 'displaced vortex' regime, in which the regular monopole's center is offset from the singular vortex position, leading to their joint northwestward propagation.

The singular-vortex trajectories tend to become more zonally-oriented in the large-vortex case $L_v = 2R_d$ (**Fig. 4c.1**) and, conversely, become more meridionally-oriented in the small-vortex case $L_v = R_d/2$ (Fig. 4a.1). The small-vortex solutions are characterized by a shorter inertial stage and are only able to reach relatively small westward velocities (Fig. 4a.2) in the course of the evolution compared to the point-vortex (Fig. 4b.2) and, especially, large-vortex solutions (Fig. 4b.3), whereas the magnitudes of the meridional velocity component seem to depend more on the superviscosity K than on the size of the singular vortex, as per Figs. 4a.3, 4b.3 and 4c.3.

An interesting and somewhat unexpected property of the singular-vortex evolution is the existence of a 'post-inertial' stage of evolution in which frictional dissipation plays an important role. This stage becomes most apparent in the solutions with large K (and was not observed at all in the tiny-friction simulations); its onset can be tracked by following the evolution of the regular potential vorticity at the center of the vortex (**Fig 5**, top). In the friction-assisted steady state, regular flow is constant in the reference frame attached to the singular vortex (Fig. 5, bottom).

Fig. 4: Singular-vortex trajectories and velocities for simulations using different vortex sizes (increasing from left to right, with point-vortex case in the middle and different values of horizontal superviscosity (see legends). Trajectories become more zonal with decreasing K and increasing L_v.

Fig. 5: Friction-assisted steady state (large K). Top: evolution of the regular potential vorticity $q=\Omega(\mathbf{r}=\mathbf{r}_0)+\beta y_0$ at the center of the vortex (which is a conserved quantity in the inviscid case (Reznik 1992). In the friction-assisted steady state, Ω remains constant in the reference frame associated with the singular vortex, and q increases with time as βy_0. Bottom: regular streamfunction (left) and potential vorticity $\Omega+\beta y$ (right) in the vicinity of the singular vortex in the friction-assisted steady-state regime. Note the singular vortex position (black dot) is offset from the streamfunction maximum, leading to the system's northwestward propagation.

Discussion

In this work, we developed a numerical formulation to approximate the evolution of an individual singular vortex under beta-plane quasi-geostrophic dynamics and demonstrated that our numerical scheme provides a faithful replica of the inviscid continuous equations, as well as of its modifications in the presence of friction. Our numerical procedure can be readily generalized to the case of any number of singular vortices interacting with one another and with the regular flow. Using this numerical model, we examined the flow development at large times, beyond the well-studied linear regime characterized by the formation of the regular field's 'beta-gyres' dipole, which forces the singular cyclone to move northwestward. We showed that, as the self-interactions of the regular field become important, beta gyres disintegrate and a different, new mechanism of the singular vortex's self-propelled motion comes into play. Furthermore, for large friction, the inertial stage is followed by the frictional regime culminating in friction-assisted steady state (cf. Early et al. 2011).

These results lay a foundation for numerical consideration of systems of multiple singular vortices, which could provide further insights in our fundamental understanding of the processes underlying the multi-scale atmospheric variability.

References

Early et al., 2011, J. Phys. Ocean., 41, 1535–1554.

Gryanik, 1986, Okeanologiya, 26, 174-179. (Oceanology, 26, 126.)

Kravtsov and Gulev, 2013, J. Atmos. Sci., 70, 2574–2595.

Kravtsov et al. 2015, J. Atmos. Sci., 72, 487–506.

Löptien and Ruprecht, 2005, Mon. Wea. Rev., 133, 2894–2904.

Morikawa, 1960, J. Met., 17, 148.

Obukhov, 1949, Izv. Acad. Nauk SSSR, Geograph., 8, 281.

Reznik, 1992, J. Fluid Mech., 240, 405–432.

Acknowledgments

For further information

Please contact kravtsov@uwm.edu. A PDF version of this poster can be found at the Sergey Kravtsov's UWM website — https://people.uwm.edu/kravtsov/presentations/